Enterococcus faecalis demonstrates pathogenicity through increased attachment in an *ex vivo* polymicrobial pulpal infection

Wayne Nishio Ayre,[a]# Genevieve Melling,[a] Camille Cuveillier,[a] Madhan Natarajan,[a] Jessica L. Roberts,[a+] Lucy L. Marsh,[a] Christopher D. Lynch,[b] Jean-Yves Maillard,[c] Stephen P Denyer,[d] Alastair J. Sloan[a]

[a] School of Dentistry, Cardiff University, Cardiff, UK.

[b] University Dental School & Hospital, University College Cork, Cork, Ireland

[c] School of Pharmacy and Pharmaceutical Sciences, Cardiff University, Cardiff, UK

[d] School of Pharmacy and Biomolecular Sciences, University of Brighton, Brighton, UK

Running Head: *E. faecalis* pulpal pathogenicity and attachment

#Address correspondence to Wayne Nishio Ayre, ayrewn@cardiff.ac.uk

[+]Present address: North Wales Centre for Primary Care Research, Bangor University, Bangor, UK

Abstract

This study investigated the host response to a polymicrobial pulpal infection consisting of *Streptococcus anginosus* and *Enterococcus faecalis*, bacteria commonly implicated in dental abscesses and endodontic failure, using a validated *ex vivo* rat tooth model. Tooth slices were inoculated with planktonic cultures of *S. anginosus* or *E. faecalis* alone or in co-culture at ratios of 50:50 and 90:10 *S. anginosus* to *E. faecalis*. Attachment was semi-quantified by measuring area covered by fluorescently labelled bacteria. Host response was established by viable histological cell counts and inflammatory response using RT-qPCR and immunohistochemistry. A significant reduction in cell viability was observed for single and polymicrobial infections, with no significant differences between infection types ($\approx$2000cells/mm^2 for infected pulps compared to $\approx$4000cells/mm^2 for uninfected pulps). *E. faecalis* demonstrated significantly higher levels of attachment (6.5%) compared to *S. anginosus* alone (2.3%) and mixed species infections (3.4% for 50:50 and 2.3% for 90:10), with a remarkable affinity to the pulpal vasculature. Infections with *E. faecalis* demonstrated the greatest increase in TNF-α (47.1 fold for *E. faecalis*, 14.6 fold for *S. anginosus*, 60.1 fold for 50:50 and 25.0 fold for 90:10) and IL-1β expression (54.8 fold for *E. faecalis*, 8.8 fold for *S. anginosus*, 54.5 fold for 50:50 and 39.9 fold for 90:10) when compared to uninfected samples. Immunohistochemistry confirmed this with the majority of inflammation localised to the pulpal vasculature and odontoblast regions. Interestingly, *E. faecalis* supernatant and heat killed *E. faecalis* treatment was unable to induce the same inflammatory response, suggesting *E. faecalis* pathogenicity in pulpitis is linked to its greater ability to attach to the pulpal vasculature.

Introduction

The dental pulp is a complex environment composed of soft connective tissue, nerves, blood vessels and a variety of cells, such as dental pulp stem cells, fibroblasts and odontoblasts (1). When the pulp becomes inflamed in response to bacterial infection or other stimuli, this is known as pulpitis. Early stages are considered “reversible” and treatment involves removal of the stimulus, such as carious lesions, in order to maintain pulp vitality. If untreated however, the microbial invasion may progress into the deeper dentin and subsequently the pulpal chamber resulting in severe tissue degradation and necrosis. This condition, known as “irreversible pulpitis”, requires a challenging and difficult endodontic or root canal treatment, which involves the removal of the pulp and obturation with an inert material. The success rate of root canal treatments is highly variable, ranging from 31% to 96% depending on clinical considerations (2) and studies across a range of countries have shown a high percentage (up to 67.9%) of patients who have undergone this treatment subsequently develop apical periodontitis (3, 4). An alternative endodontic treatment is vital pulpotomy, which involves removal of the coronal pulp, leaving the radicular pulp vital and free of any pathological alterations (5). Although this procedure is thought to require shorter appointment times and can be accomplished in one visit, the efficacy of this technique is debated with success rates of clinical studies ranging from 70% to 96% (6). Accurate models to better understand the process of pulpal infection and to test the efficacy of novel therapeutics will aid in the development of more effective vital pulp treatments. *In vitro* monolayer cell culture models lack the complexity of the pulpal matrix, whilst *in vivo* studies suffer from systemic factors, high costs and ethical considerations. To overcome these limitations, Roberts et al. (7) developed an *ex vivo* co-culture

system to model pulpal infections on rat tooth slices. This study focused predominantly on the *Streptococcus anginosus* group (SAG), consisting of *S. anginosus, S. constellatus* and *S. intermedius*, Gram-positive cocci which are part of the body's commensal flora. This group are known to be primary colonisers of the oral cavity due to their ability to attach to the salivary pellicle and other oral bacteria (8). They are considered opportunistic pathogens and have been reported to form dental abscesses (9). The study by Roberts et al. demonstrated a significant reduction in viable pulp cells, an increase in cytokine expression and bacterial attachment over 24 hours as a result of *S. anginosus* infections (7).

Although Roberts et al. demonstrated invasion of the dental pulp by *S. anginosus* group species, the number of microbial species encountered in the oral cavity is far more diverse, with studies identifying between 100 to 300 different species from different regions of the oral cavity of healthy individuals (10). It is therefore unsurprising that complex mixed species microbiomes are often detected in cases of pulpitis (11). As lesions progress into the tooth, a shift in microbial species has been well documented due to environmental and nutritional changes (12). Of particular interest is the *Enterococcus faecalis* species, a Gram-positive facultative anaerobic coccus, also part of the normal human commensal flora (13). *E. faecalis* has been shown to be pathogenic, particularly in endodontic failure (14) with prevalence in such infections ranging from 24% up to 77% (15). Although highly implicated in persistent endodontic failure, molecular studies have recently revealed this species is frequently present in necrotic pulps, highlighting its potential role in late-stage pulpitis (16, 17).

This study aims to use a validated *ex vivo* co-culture model to quantify and better understand the host tissue response to mixed species pulpal infections

caused by *S. anginosus* and *E. faecalis*. Understanding the mechanism of complex pulpal infections and the host inflammatory response may elucidate potential targets for more effective vital pulp therapies.

Results

Mixed species culture does not significantly influence S. anginosus and E. faecalis growth rate.

Growth characteristics in a simple mixed species planktonic broth culture were investigated to ensure potential competitive growth between *S. anginosus* and *E. faecalis* would not influence the *ex vivo* experiments investigating host tissue response.

Clinical isolates of *S. anginosus* and *E. faecalis* species were selected from the culture collection of the Oral Microbiology Unit, School of Dentistry at Cardiff University. Species identity was confirmed by standard microbial identification tests and 16S rRNA sequencing as described in the methods and supplemental materials (Fig. S1 and S2).

Fig. 1 shows the planktonic growth curves for *S. anginosus* and *E. faecalis* alone and in combination at ratios of 50:50 and 90:10 respectively over 24 hours in BHI. *E. faecalis* reached mid-log phase earlier than *S. anginosus* (8 hours for *E. faecalis* compared to 10 hours for *S. anginosus*). When cultured at a ratio of 50:50 however, *S. anginosus* reached mid-log at a similar time to *E. faecalis* (10 hours). When the bacteria were cultured at an *S. anginosus* to *E. faecalis* ratio of 90:10, *S. anginosus* reached mid-log at approximately 8 hours and *E. faecalis* at approximately 12 hours. Growth rate calculations during the log phase demonstrated no significant

differences between *E. faecalis* and *S. anginosus* under all culture conditions (p>0.05, Table 1).

E. faecalis demonstrates greater levels of attachment to dental pulp than S. anginosus at 24 hours, with particular affinity to the pulpal vasculature.

To assess differences in bacterial attachment to the dental pulp, the *ex vivo* rat tooth model was infected with planktonic cultures of *S. anginosus* and *E. faecalis* individually or as mixed species infections. Gram staining and fluorescent labelling of bacteria were undertaken to localise and semi-quantify bacterial attachment.

High levels of bacterial attachment to the pulp were detected for tooth slices incubated with *E. faecalis* (Fig. 2A) and mixed species of *S. anginosus* and *E. faecalis* (Fig. 2B to 2C). Attachment was predominantly observed in intercellular spaces within the pulpal matrix and around the pulpal vasculature. Bacteria were also observed attached to soft tissue surrounding the tooth and within dentinal tubules (Fig. 2D and 2E). Attachment of bacteria was not detected using Gram staining on tooth slices incubated with *S. anginosus* alone.

Control samples demonstrated low levels of background fluorescence (Fig. 3A). Infections consisting of *E. faecalis* alone had the greatest fluorescent signal, in particular centred near the pulpal vasculature (Fig. 3B). *S. anginosus* demonstrated low bacterial attachment, spread evenly across the pulp (Fig. 3C). When combining *E. faecalis* and *S. anginosus,* higher levels of attachment were observed compared to *S. anginosus* alone (Fig. 3D to 3E), with attachment again localised predominantly to the pulpal vasculature. When the percentage bacterial coverage was semi-quantified (Fig. 3F), the single species *E. faecalis* infection had significantly higher levels of bacterial attachment when compared to *S. anginosus* alone (approximately

6.5% compared to 2%, p=0.00021) and the mixed species infections (50:50, p=0.0235 and 90:10, p=0.0032).

S. anginosus and E. faecalis infections significantly reduce pulp cell viability with E. faecalis infections inducing a significantly greater inflammatory response.

To establish the dental pulp host response to *S. anginosus* and *E. faecalis* infections alone and as mixed species infections, histomorphometric analysis was performed alongside RT-qPCR and immunohistochemistry for TNF-α and IL-1β expression.

Histological cell counts of the infected tooth sections demonstrated a significant reduction ($p \leq 0.05$) in viable cells due to infection by both *E. faecalis* and *S. anginosus* alone and in combination (Fig. 4A). There were no significant differences in cell numbers between single species infections and multi-species infections.

All infected samples had significantly higher pro-inflammatory cytokine expression, tumour necrosis factor alpha (TNF-α, Fig. 4B) and interleukin 1 beta (IL-1β, Fig. 4C), when compared to the control samples ($p \leq 0.05$). The single species infection of *E. faecalis* resulted in significantly higher levels of TNF-α and IL-1β expression when compared to *S. anginosus* (p=0.0276 and p=0.0234 for TNF-α and IL-1β respectively). Combining *E. faecalis* and *S. anginosus* together did not result in a significantly higher inflammatory response from the pulp when compared to *E. faecalis alone* (for TNF-α p=0.493 and p=0.096 for 50:50 and 90:10 respectively and for IL-1β p=0.988 and p=0.400 for 50:50 and 90:10 respectively).

Negative controls replacing the primary TNF-α antibody with a nonimmune immunoglobulin G control showed no immunopositivity (Fig. S3). Similarly, primary exclusion controls were negative for staining, indicating specific binding of the

secondary antibody (Fig. S3). Control samples demonstrated low expression of TNF-α and interestingly *S. anginosus* alone did not induce a high TNF-α response (Fig. 4D). Samples incubated with *E. faecalis* alone or in combination with *S. anginosus* had the most pronounced staining, both within the pulp (around the vasculature) and the odontoblast layer. The level of TNF-α staining in these samples was similar to those encountered in the rat lung positive control (Fig. S3).

Immunohistochemistry staining for IL-1β, showed no positive signal for IgG and primary exclusion controls (Fig. S3). Similar to the TNF-α immunohistochemistry, the control sample and the sample incubated with *S. anginosus* alone had few positively stained cells, whilst samples incubated with *E. faecalis* alone and in combination with *S. anginosus* had more positively stained cells (Fig. 4D). Although the level of staining was not as pronounce as observed with TNF-α, the positive cells were again located adjacent to the pulpal vasculature and similar in staining to the positive lung control (Fig. S3).

Greater host inflammatory response to E. faecalis is not due to differences in water soluble cell wall proteins or culture supernatants.

To establish whether the increased host inflammatory response to *E. faecalis* was due to specific water soluble cell proteins or components of the culture supernatant, SDS-PAGE was performed to identify proteins in water soluble cell wall proteins and culture supernatants. Similarly, heat killed *E. faecalis* and *E. faecalis* supernatant was used to stimulate the pulp in order to assess the host response.

Few differences were observed between the water soluble cell wall proteins of *S. anginosus* and *E. faecalis* when cultured alone and in combination with each other (Fig. S4A). In terms of the culture supernatant, there was one band at approximately

35kDa observed with the *E. faecalis* cultures that was not observed with *S. anginosus* (Fig. S4B).

When culturing the rat tooth slices with the *E. faecalis* supernatant or the heat killed *E. faecalis*, no significant differences were observed in TNF-α expression when compared to the untreated controls (Fig. 5A, p=0.196 and p=0.152 for supernatant and heat killed *E. faecalis* respectively). A significant increase was observed in IL-1β expression for the tooth slices cultured with heat killed *E. faecalis* when compared to the untreated controls (Fig. 5B, p=0.041) but not for *E. faecalis* supernatant (p=0.148).

The negative controls (IgG control and primary exclusion) and the control sample for the TNF-α immunohistochemistry did not show staining (Fig. S5). The tooth slices incubated with *E. faecalis* supernatant had few cells stained positive for TNF-α, the majority of which was concentrated at the pulpal vasculature and odontoblast layer (Fig. 5C). Similarly, the heat-killed *E. faecalis* had few cells expressing TNF-α (Fig. 5C), whilst the lung positive control stained positive for TNF-α (Fig. S5).

The IgG control, the primary exclusion control and the untreated sample (Fig. S5) did not stain positive for IL-1β. Fewer cells were positive for IL-1β than TNF-α (Fig. 5C). Samples treated with *E. faecalis* supernatant showed some cells stained positive within the pulpal vasculature, whilst heat-killed *E. faecalis* showed few positively stained cells. The positive lung control demonstrated cells stained positive for IL-1β expression (Fig. S5).

Discussion

This study has successfully employed an existing *ex vivo* rat tooth infection model to study the effect of mixed species *E. faecalis* and *S. anginosus* pulpal infections on cell viability, bacterial attachment and host inflammatory response.

By studying simple planktonic growth kinetics, it was established that *E. faecalis* caused the *S. anginosus* bacteria to reach log phase at a more rapid rate. This concept of polymicrobial synergy has been highlighted in recent work, which investigated metabolite cross-feeding, whereby metabolic end-products produced by one bacterium are consumed by a second community member (18-20). In particular, this has been demonstrated for a similar oral pathogen, *Streptococcus gordonii.* Lactate produced by *S. gordonii* as the primary metabolite during catabolism of carbohydrates was found to support the growth of *Aggregatibacter actinomycetemcomitans* (20). Interestingly, in a study using a primate model, the addition of *E. faecalis* to a four-strain mixed species culture resulted in higher levels of survival of all four bacteria than in the absence of *E. faecalis* (21). Another mechanism of coordinating activities and communicating between microbial species is quorum sensing, which has been shown to occur between different groups of Streptococci (22). Although the rate of growth during the log phase was not altered during mixed species planktonic culture in this study, it is important to appreciate that under mixed species biofilm conditions, alterations in growth are likely to occur.

The mixed species infection did not result in higher levels of bacterial attachment when compared to *E. faecalis* alone. The data suggests that *E. faecalis* is capable of attaching to the dental pulp to a greater extent than *S. anginosus*, with a particular affinity to the pulpal vasculature. This was not attributed to a more rapid rate of growth or higher number of bacteria as a similar number of *S. anginosus* was

counted after 24 hours in planktonic broth culture. Similarly in the mixed species culture where *S. anginosus* achieved log phase at an earlier time point, attachment was not as high when compared to *E. faecalis* alone. The increased attachment may therefore be due to differences between the species in terms of motility, sensing or cell surface adhesins. *E. faecalis* and *S. anginosus* are classified as groups D and F respectively using Lancefield grouping (23), a method of grouping based on the carbohydrate antigens on the cell wall. These differences in surface carbohydrates could mediate changes in attachment to epithelial cells as demonstrated by Guzman et al. (24). A review by Fisher and Phillips (25) highlighted *E. faecalis* specific cell wall components which play a vital role in pathogenic adhesion. Aggregation substance (Agg) increases hydrophobicity and aids adhesion to eukaryotic and prokaryote surfaces and also encourages the formation of mixed-species biofilm through adherence to other bacteria. Extracellular surface protein (ESP) promotes adhesion, antibiotic resistance and biofilm formation. Adhesin to collagen of *E. faecalis* (ACE) is a collagen binding protein belonging to the microbial surface components recognizing adhesive matrix molecules (MSCRAMM) family. ACE plays a role in the pathogenesis of endocarditis and *E. faecalis* mutants which do not express ACE have been shown to have significantly reduced attachment to collagens type I and IV but not fibrinogen (26, 27). Whilst *S. anginosus* has been shown to adhere to the extracellular matrix components fibronectin, fibrinogen and laminin, binding to collagens type I and IV was much less prominent (28). This is of particular interest in explaining differences in pulpal adherence and the affinity of *E. faecalis* to localise near the pulpal vasculature, as collagen fibres are often found in higher density around blood vessels and nerves (29).

Although the level of cell death was the same between the groups tested, infections consisting of *E. faecalis* alone produced a greater inflammatory response when compared to *S. anginosus* and mixed species infections. This increase in inflammation was not due to supernatant or water-soluble cell wall virulence factors of *E. faecalis* as treatment of the dental pulp with these isolated factors did not yield high levels of TNF-α and IL-1β expression both at gene and protein level. Basic analysis of supernatant and water soluble cell-wall proteins by SDS-PAGE showed similar bands, however this may be due to the absence of serum or collagen (present in the co-culture model) which has been shown to influence virulence factor production, such as ACE (27). These results indicate the pulpal inflammation caused by *E. faecalis* is likely due to the higher levels of attachment to the dental pulp. Similar pathogenic traits have been established for *E. faecalis* in urinary tract infections and endocarditis (30). Increased attachment to the dental pulp would allow direct contact between cells and cell wall components such as lipoteichoic acid (LTA), which induces activation of cluster of differentiation 14 (CD-14) and toll-like receptor 2 (TLR-2) (31). An *in vivo* study, which infected canine pulp with lipopolysaccharides (LPS) from *Escherichia coli* and lipoteichoic acid (LTA) from *E. faecalis,* demonstrated LTA treatment led to pulp destruction, albeit to a lesser extent than LPA (32). *In vitro* studies investigating macrophage responses to *E. faecalis* LTA found that TNF-α expression was significantly increased in a dose-dependent manner (33), with one study attributing it to the NF-κB and p38 MAPK signalling pathways (34). These studies however were performed using monolayer cultures, allowing easy access for LTA to activate toll-like receptors, whereas the presence extracellular matrix would limit penetration of virulence factors into the dental pulp *in vivo*. Furthermore macrophages are normally present as monocytes in normal

297 healthy pulp and require a stimulus to become activated (35). Studies using
298 immunohistochemistry have shown these monocytes as well as dendritic cells to be
299 located predominantly around blood vessels, with few distributed throughout the pulp
300 (36, 37).

301 High levels of TNF-α expression were also observed in the odontoblast region
302 using immunohistochemistry. Due to its anatomical location, odontoblasts are the
303 first cells to encounter foreign antigens either through infiltration of virulence factors
304 through dentinal tubules or the breakdown of enamel and dentine. Through Gram
305 staining in this study, *E. faecalis* was observed within the dentinal tubules of the
306 infected tooth slices. This phenomenon has been previously reported in human
307 teeth (38). Odontoblasts, which line the dentine, have been shown to express TLRs
308 and play a role in the pulp's immune response, in particular to bacterial exotoxins
309 (39-41). This explains the high inflammatory response observed for both infections
310 and supernatant treatments when assessed using immunohistochemistry. Cytokine
311 gene expression using RT-qPCR however did not demonstrate higher levels when
312 treating the dental pulp with supernatants or heat killed bacteria. This may be
313 attributed to the fact that the methods employed for pulp extraction would be unlikely
314 to fully remove the odontoblast cells.

315 Although the host response to a mixed species infection consisting of *S.*
316 *anginosus* and *E. faecalis* has been established and the potential pathogenicity of *E.*
317 *faecalis* in pulpal infections has been elucidated, there are several limitations to this
318 study. The methods employed to fluorescently localise the bacteria could potentially
319 result in diffusion-related artefacts. More specific post-processing techniques, such
320 as fluorescent in-situ hybridization (FISH) probes may allow for more specific
321 identification, quantification and localisation of mixed species pulpal infections.

Whilst the *ex vivo* model offers a 3D organotypic culture setting, the static nature, which lacks blood flow does not allow full observation of the systemic immune response. Potential methods to overcome this may involve addition of monocytes directly to the culture media and prolonged incubation times to stimulate repair mechanisms. Closer examination of attachment mechanisms using ACE negative *E. faecalis* mutants and purified LTA would also help fully establish the pathogenicity of *E. faecalis* in pulpal infections. This will allow the model to be used to develop more effective treatments for pulpitis by assessing the efficacy of antimicrobial and anti-inflammatory treatments to inhibit bacterial colonisation.

In conclusion, this study has modelled a mixed species pulpal infection consisting of *S. anginosus* and *E. faecalis* using a validated *ex vivo* rat tooth model. Although *E. faecalis* caused *S. anginosus* to reach log growth phase more rapidly, the mixed species infection did not result in higher cell death, attachment or inflammatory response from the dental pulp. *E. faecalis* was found to elicit a much greater inflammatory response, which was due to higher levels of attachment to the dental pulp, with a particular affinity to the pulpal vasculature. Future work will focus on assessing the mechanisms and attachment kinetics in order to elucidate the molecular process and rate at which *E. faecalis* colonises the pulp.

Materials and Methods

Materials

All reagents including culture media, broths and agars were purchased from Thermo Scientific (Leicestershire, UK) unless otherwise stated.

Bacterial identification

347 The *S. anginosus* and *E. faecalis* species studied were clinical isolates selected
348 from the culture collection of the Oral Microbiology Unit, School of Dentistry at Cardiff
349 University. To confirm the identity of the species, standard microbial identification
350 tests were performed by assessing: colony appearance on blood agar, Gram
351 staining, haemolysis, presence of catalase, lactose fermentation (MacConkey agar),
352 Lancefield grouping and bile aesculin agar growth.
353 16S rRNA sequencing was also performed on the *S. anginosus* and *E. faecalis*
354 clinical isolates to validate species identity. *S. anginosus* and *E. faecalis* were
355 cultured overnight in brain heart infusion (BHI) broth at 37°C, 5% CO_2. DNA was
356 extracted from using a QIAamp DNA Mini Kit (Qiagen, Manchester, UK), according
357 to the manufacturer's instructions. DNA was used in a PCR reaction using 16S
358 rRNA bacterial universal primers D88 (F primer; 5'-GAGAGTTTGATYMTGGCTCAG-
359 3') and E94 (R primer; 5'-GAAGGAGGTGWTCCARCCGCA-3') (42) and sequencing
360 of the products was performed by Central Biotechnology Services (Cardiff University)
361 using a 3130xl Genetic Analyser (Applied Biosystems). DNA sequences were
362 aligned with GenBank sequences using BLAST (NCBI) to establish percentage
363 sequence identity.
364
365 *Growth curves*
366 Overnight cultures of *S. anginosus* and *E. faecalis* in BHI broth were prepared
367 and diluted to 10^8 colony forming units/mL (CFU/mL, absorbance at 600nm=0.08-
368 0.1). The inoculum was diluted in BHI to give a starting concentration of 10^2
369 CFU/mL. Mixed species planktonic cultures with a total of 10^2 CFU/mL were
370 prepared consisting of 50% *S. anginosus* and 50% *E. faecalis* (herein referred to as
371 50:50) and 90% *S. anginosus* and 10% *E. faecalis* (herein referred to as 90:10). The

broths were incubated at 37°C, 5% CO_2 and 1mL aliquots removed every 4 hours for 24 hours. The absorbance of the aliquots was measured at 600nm using an Implen OD600 DiluPhotometer (München, Germany) and 50µL spiral plated on tryptic soya agar using a Don Whitley Automated Spiral Plater (West Yorkshire, UK). The remaining aliquot was then heat treated at 60°C for 30 minutes prior to spiral plating on bile aesculin agar containing 6.5%w/w sodium chloride. Heat treatment and the presence of high concentrations of bile and sodium chloride would only permit the growth of *E. faecalis* but not *S. anginosus* (43). Plates were incubated at 37°C, 5% CO_2 for 24 hours prior to counting. *E. faecalis* counts were subtracted from total counts to give the number of *S. anginosus* bacteria. Specific growth rate was calculated using the log phase of each growth curve and Equation 1, where µ is the growth rate in CFU/mL per hour, x is the CFU/mL at the end of the log phase, x_o is the CFU/mL at the start of the log phase and t is the duration of the log phase in hours.

$$\mu = \frac{\ln(x - x_o)}{t} \quad [1]$$

Co-culture model

The co-culture rat tooth infection model was prepared as described by Roberts et al. (7). 28-day-old male Wistar rats were sacrificed under schedule 1 of the UK Animals Scientific Procedures Act, 1986 by a qualified technician at the Joint Biological Services Unit, Cardiff University for harvesting of tissue. Upper and lower incisors were extracted and the incisors were cut into 2mm thick transverse sections using a diamond-edged rotary bone saw (TAAB, Berkshire, UK). The sections were transferred to fresh sterile Dulbecco's Modified Eagle Medium (DMEM) for no more than 20 minutes before being cultured in 2mL DMEM, supplemented with 10%v/v

heat-inactivated fetal calf serum, 0.15mg/mL vitamin C, 200mmol/L L-glutamine, 100U/mL penicillin, 100µg/mL streptomycin sulphate and 250ng/mL amphotericin B at 37°C, 5% CO_2 for 24 hours. Tooth slices were then washed in 2mL of phosphate buffered saline (PBS), transferred to supplemented DMEM without antibiotics and incubated overnight to remove traces of antibiotic. *S. anginosus* 39/2/14A and *E. faecalis* were cultured to the log phase in BHI for 8-12 hours before dilution to 10^2 CFU/mL in BHI. The bacteria were then used alone or combined for mixed species infections (*S. anginosus* to *E. faecalis* ratios of 50:50 and 90:10 respectively). Forty µL of 1%w/v fluorescein diacetate (FDA) in acetone was added to 2mL of the bacterial suspension and incubated for 30 minutes at 37°C, 5% CO_2 before being passed through a 0.22µm syringe-driven filter unit (Millipore, Oxford, UK). Bacteria captured on the filter were then resuspended in 2mL sterile supplemented DMEM without antibiotics and with 10%v/v BHI (herein referred to as DMEM-BHI) and used to inoculate one tooth slice. Tooth slices were incubated with the bacteria at 37°C, 5% CO_2 for 24 hours under constant agitation at 60rpm in the dark. Sterile DMEM-BHI was used as a control. After incubation the tooth slices were processed for histology in the dark. Tooth slices were fixed in 10%w/v neutral-buffered formalin at room temperature for 24 hours. Slices were demineralized in 10%w/v formic acid at room temperature for 72 hours; dehydrated through a series of 50%v/v, 70%v/v, 95%v/v, and 100%v/v ethanol followed by 100%v/v xylene for five minutes each; and embedded in paraffin wax. Sections 5µm thick were cut and viewed under a fluorescent microscope with a FITC filter, with images captured using a Nikon digital camera and ACT-1 imaging software (Nikon UK Ltd, Surrey, UK). To quantify cell viability and structural degradation, sections were stained with hematoxylin and eosin (H&E) prior to capturing images with a light microscope.

Gram stain of tissue sections

Gram stains of tooth slices were performed using a modified Brown and Brenn method (44). Paraffin-embedded tooth slices were cut using a microtome into 5µm sections and rehydrated through a series of xylene, 100, 95 and 70%v/v ethanol for five minutes each. Sections were immersed in 0.2%w/v crystal violet for 1 minute, rinsed with distilled water, immersed in Gram's iodine for 1 minute, rinsed with distilled water, decolourised with acetone for 5 seconds and counterstained for 1 minute with basic fuchsin solution prior to washing with distilled water and mounting. Light microscopy images were captured at x100 magnification using a Nikon digital camera and ACT-1 imaging software (Nikon UK Ltd, Surrey, UK).

Semi-quantification of cell viability by cell counts

ImageJ (National Institutes of Health, Maryland USA) was used to count the number of nuclei per pulp on stained histological sections. For each time point, sections were cut from 5 tooth slices. Images were captured at x20 magnification and combined using ImageJ software (Fig. S6). The blue field was extracted from the images and the moments threshold method was applied to separate the pulp cells. The watershed function was applied to split adjacent cell nuclei and the number of particles ranging in size from 3 to 100µm^2 were counted. The data was normalised to the pulpal area and standard errors of the mean were calculated.

Semi-quantification of bacterial coverage

ImageJ was used to quantify the area of the pulp inoculated with fluorescent bacteria. The green field of the fluorescent image was extracted and the image

converted into a binary form using the moments threshold method. The pulpal area was manually selected and the total area of the pulp measured. The area covered by the fluorescent bacteria was then measured and calculated as a percentage of the selected pulp area (Fig. S7).

RT-qPCR of cytokines

Four mm thick tooth slices were cultured as previously described for 24 hours with either sterile DMEM-BHI as a control; DMEM-BHI inoculated with 10^2CFU/mL *S.anginosus* or *E. faecalis* or DMEM-BHI with a mixed species of *S.anginosus* or *E. faecalis* (50:50 and 90:10 ratios respectively). After incubation, the tooth slice was transferred to sterile PBS and the pulp removed by flushing the pulpal cavity with PBS using a 0.1mm needle and syringe. RNA was extracted using TRIzol® Reagent (ThermoFisher Scientific, Loughborough, UK) followed by RNAse treatment (Promega, Southampton, UK) according to the manufacturers' instructions.

Analysis of gene expression was performed in accordance to the Minimum Information for publication of Quantitative real-time PCR Experiments (MIQE) guidelines (45). RNA concentrations were determined using a NanoVue Spectrophotometer (GE Healthcare Life Sciences, Buckinghamshire, UK). RNA purity was determined by ensuring the ratio of absorbance at 260/280nm was above 1.8 and RNA quality checked by separating 1µg of RNA electrophoretically on a 2% agarose gel containing SafeView (NBS Biologicals, Cambridgeshire, UK) in Tris/Borate/EDTA buffer to ensure intact 28S and 18S rRNA bands using a Gel Doc™ EZ System (BioRad, Hertfordshire, UK). Fig. S8 demonstrates RNA integrity following extraction for samples tested.

Complementary DNA (cDNA) was synthesized by reverse transcription using Promega reagents (Southampton, UK) in a G-Storm GS1 thermocycler (Somerton, UK). One µg extracted RNA was combined with 1µL random primer in a 15µL reaction in nuclease free water at 70°C for 5 minutes. This suspension was added to 5µL MMLV reaction buffer, 1.25µL deoxyribonucleotide triphosphates (10mM stock dNTPSs), 0.6µL RNasin, 1µL MMLV enzyme and 2.15µL nuclease free water and incubated at 37°C for 1 hour.

The resultant cDNA was diluted 1:10 in nuclease free water (25ng cDNA). Forward and reverse primers used are listed in Table 2. Ten µL of PrecisionFAST qPCR SYBR Green MasterMix with low ROX (Primerdesign, Chandler's Ford, United Kingdom) was combined with 2µL of forward and 2µL of reverse primers (3µM) with 1µL nuclease-free water prior to addition of 5µL cDNA in BrightWhite Real-time PCR FAST 96-well plates (Primerdesign, Chandler's Ford, United Kingdom). The plates were subsequently heated to 95°C for 20 seconds; then 40 cycles of: 95°C for 1 second and 55°C for 20 seconds; followed by melt-curve analysis at 95°C for 15 seconds, 60°C for 60 seconds and 95°C for 15 seconds in a QuantStudio™ 6 Flex Real-Time PCR System with QuantStudio Real-Time PCR Software (ThermoFisher Scientific, Loughborough, UK). Relative TNF-α and IL-1β gene expression was calculated with beta actin (β-actin) as the reference gene and uninfected samples as the control using the Livak method (46).

Primer specificity was ensured by the presence of single melt curve peaks (Fig. S9) and by running products on agarose gels, as previously described, to confirm single bands and correct product lengths (Fig. S10). Primer efficiency was between 90-110% for all primers used (Fig. S11) and determined using total rat RNA converted to cDNA, as previously described, and serially diluted 1:4 in nuclease-free

water. Reference gene validation was performed by comparing gene stability across all samples using NormFinder software (47). β-actin was found to be the most stable reference gene (Fig. S12).

TNF-α and IL-1β Immunohistochemistry

Immunohistochemical staining of the tooth slices for TNF-α and IL-1β was performed based on methods used by Smith et al (48). Rat lung was used as a positive control for TNF-α and IL-1β following fixation in 10%w/v neutral-buffered formalin at room temperature for 24 hours, dehydration through a series of 50%v/v, 70%v/v, 95%v/v, and 100%v/v ethanol followed by 100%v/v xylene for five minutes each; and embedding in paraffin wax. Paraffin-embedded tooth slices and lung samples were cut using a microtome into 5 μm sections and incubated on glass slides at 65°C for one hour. The samples were subsequently rehydrated through a series of xylene, 100%v/v, 95%v/v and 70%v/v ethanol and double-distilled water for 5 minutes each. Endogenous peroxidase activity within the tissue sections was quenched by incubation in 3%w/v hydrogen peroxide for 10 minutes, followed by 2 washes for 2 minutes in tris-buffered saline (TBS). Non-specific binding was blocked with 3%v/v normal horse serum (Vector laboratories, Peterborough, UK) in TBS for 30 minutes. Sections were incubated for 1 hour with primary antibodies for TNF-α and IL-1β (Santa Cruz Biotechnology, Heidelberg, Germany) diluted 1:50 in TBS containing 1%w/v bovine serum albumin (Sigma Aldrich, Gillingham, UK). Immunoreactivity was then performed using a Vectastain ABC peroxidase detection kit (Vector laboratories, Peterborough, UK). Negative controls included omission of the primary antibody and replacements of the primary antibody with immunoglobulin G isotype diluted to the working concentration of the primary antibody. Sections

were counterstained with 0.05% light green for 30 seconds, dehydrated with 100% ethanol and xylene for 10 minutes each and mounted using VectaMount Permanent Mounting Medium (Vector laboratories, Peterborough, UK) prior to imaging using a Nikon digital camera and ACT-1 imaging software (Nikon UK Ltd, Surrey, UK).

SDS-PAGE of bacterial proteins

An overnight culture of *S. anginosus* and *E. faecalis* in BHI was prepared and diluted to 10^2 CFU/mL. *S. anginosus* and *E. faecalis* were cultured at 37°C, 5% CO_2 for 24 hours alone or in combination at a ratio of 50:50 and 90:10 respectively. The suspensions were centrifuged at 5000g for 5 minutes. The supernatant was used for analysis of supernatant proteins. The pellet was lysed in RIPA buffer by vortexing for 30 seconds followed by 30 seconds ultrasonication at 50 Joules using a Branson SLPe sonifier (Connecticut, USA). Protein concentrations in the supernatant and the bacterial pellet were quantified using a BCA assay (ThermoFisher Scientific, Loughborough, UK) and 20µg of protein in Laemmli buffer (Biorad, Hertfordshire, UK) separated by SDS-PAGE at 200V for 40 minutes. Gels were stained using a Biorad Silver Stain Plus Kit according to the manufacturer's instructions and imaged using a Gel Doc™ EZ System (Biorad, Hertfordshire, UK).

E. faecalis supernatant and heat-killed *E. faecalis* treatments

An overnight culture of *E. faecalis* was diluted in 20mL DMEM-BHI media to give a starting inoculum of 10^2CFU/mL as previously described. After incubation for an additional 24 hours at 37°C, 5% CO_2, the suspension was centrifuged at 5000g for 5 minutes. The supernatant was filtered through a 0.22µm syringe filter and frozen overnight at -20°C before freeze drying for 24 hours using a ScanVac CoolSafe

freeze dryer (LaboGene, Lynge, Denmark). The pellet of bacteria was resuspended in 20mL of PBS and centrifuged at 5000g for 5 minutes. This step was repeated again to ensure minimal carryover of culture supernatant. The pellet was then resuspended in 20mL DMEM-BHI and heated to 100°C for one hour. The solution was then frozen overnight at -20°C before freeze drying as previously described. 20mL of sterile DMEM-BHI was also frozen and freeze dried as a control. All freeze dried samples were individually resuspended in 20mL of sterile DMEM-BHI and used to culture rat tooth slices for RT-qPCR of cytokines and immunohistochemistry of TNF-α and IL-1β as previously described.

Statistical analysis

A one-way analysis of variance (ANOVA) was performed using the data analysis package in Excel (Microsoft, Reading, UK) to determine the relative significance of the difference between the infected groups and the controls in terms of cell counts, bacterial coverage and cytokine expression. The Tukey-Kramer test was used in conjunction with ANOVA to compare the significant difference between all possible pairs of means. $P \leq 0.05$ was considered significant.

Acknowledgements

This work was supported by The Dunhill Medical Trust [grant number: R232/1111].

References

1. Nanci A. 2013. Dentin-pulp complex, p 183, Ten cate's oral histology: Development, structure, and function, 8th ed. Mosby Elsevier, St. Louis, MO.

2. Ng YL, Mann V, Rahbaran S, Lewsey J, Gulabivala K. 2007. Outcome of primary root canal treatment: Systematic review of the literature - Part 1. Effects of study characteristics on probability of success. Int Endod J 40:921-39.

3. Mukhaimer R, Hussein E, Orafi I. 2012. Prevalence of apical periodontitis and quality of root canal treatment in an adult palestinian sub-population. The Saudi Dental Journal 24:149-155.

4. Berlinck T, Tinoco JMM, Carvalho FLF, Sassone LM, Tinoco EMB. 2015. Epidemiological evaluation of apical periodontitis prevalence in an urban brazilian population. Brazilian Oral Research 29:1-7.

5. AAPD. 2016. Guideline on pulp therapy for primary and immature permanent teeth. Pediatr Dent 38:280-288.

6. Demarco FF, Rosa MS, Tarquínio SBC, Piva E. 2005. Influence of the restoration quality on the success of pulpotomy treatment: A preliminary retrospective study. Journal of Applied Oral Science 13:72-77.

7. Roberts JL, Maillard JY, Waddington RJ, Denyer SP, Lynch CD, Sloan AJ. 2013. Development of an *ex vivo* coculture system to model pulpal infection by *Streptococcus anginosus* group bacteria. J Endod 39:49-56.

8. Jenkinson HF, Demuth DR. 1997. Structure, function and immunogenicity of streptococcal antigen I/II polypeptides. Mol Microbiol 23:183-90.

9. Shweta S, Prakash SK. 2013. Dental abscess: A microbiological review. Dental Research Journal 10:585-591.

593 10. Bik EM, Long CD, Armitage GC, Loomer P, Emerson J, Mongodin EF, Nelson
594 KE, Gill SR, Fraser-Liggett CM, Relman DA. 2010. Bacterial diversity in the
595 oral cavity of ten healthy individuals. The ISME journal 4:962-974.

596 11. Rôças IN, Alves FRF, Rachid CT, Lima KC, Assunção IV, Gomes PN,
597 Siqueira JF, Jr. 2016. Microbiome of deep dentinal caries lesions in teeth with
598 symptomatic irreversible pulpitis. PLOS ONE 11:e0154653.

599 12. Hahn CL, Liewehr FR. 2007. Relationships between caries bacteria, host
600 responses, and clinical signs and symptoms of pulpitis. Journal of
601 Endodontics 33:213-219.

602 13. Suchitra U, Kundabala M. 2006. *Enterococcus faecalis:* An endodontic
603 pathogen. Endodontology 18:11-13.

604 14. Sundqvist G, Figdor D, Persson S, Sjogren U. 1998. Microbiologic analysis of
605 teeth with failed endodontic treatment and the outcome of conservative re-
606 treatment. Oral Surg Oral Med Oral Pathol Oral Radiol Endod 85:86-93.

607 15. Stuart CH, Schwartz SA, Beeson TJ, Owatz CB. 2006. *Enterococcus faecalis:*
608 Its role in root canal treatment failure and current concepts in retreatment. J
609 Endod 32:93-8.

610 16. Salah R, Dar-Odeh N, Abu Hammad O, Shehabi AA. 2008. Prevalence of
611 putative virulence factors and antimicrobial susceptibility of *Enterococcus*
612 *faecalis* isolates from patients with dental diseases. BMC Oral Health 8:17.

17. Hegde A, Lakshmi P. 2013. Prevalence of selected microorganisms in the pulp space of human deciduous teeth with irreversible pulpitis. Endodontolgy 25:107-111.

18. Brown SA, Whiteley M. 2007. A novel exclusion mechanism for carbon resource partitioning in *Aggregatibacter actinomycetemcomitans*. Journal of Bacteriology 189:6407-6414.

19. Ramsey MM, Whiteley M. 2009. Polymicrobial interactions stimulate resistance to host innate immunity through metabolite perception. Proceedings of the National Academy of Sciences 106:1578-1583.

20. Ramsey MM, Rumbaugh KP, Whiteley M. 2011. Metabolite cross-feeding enhances virulence in a model polymicrobial infection. PLOS Pathogens 7:e1002012.

21. Fabricius L, Dahlen G, Sundqvist G, Happonen RP, Moller AJ. 2006. Influence of residual bacteria on periapical tissue healing after chemomechanical treatment and root filling of experimentally infected monkey teeth. Eur J Oral Sci 114:278-85.

22. Cook LC, LaSarre B, Federle MJ. 2013. Interspecies communication among commensal and pathogenic streptococci. mBio 4.

23. Lancefield RC. 1933. A serological differentiation of human and other groups of hemolytic streptococci. The Journal of Experimental Medicine 57:571-595.

633 24. Guzmàn CA, Pruzzo C, Platé M, Guardati MC, Calegari L. 1991. Serum
634 dependent expression of *Enterococcus faecalis* adhesins involved in the
635 colonization of heart cells. Microbial Pathogenesis 11:399-409.

636 25. Fisher K, Phillips C. 2009. The ecology, epidemiology and virulence of
637 enterococcus. Microbiology 155:1749-57.

638 26. Nallapareddy SR, Qin X, Weinstock GM, Höök M, Murray BE. 2000.
639 *Enterococcus faecalis* adhesin, ace, mediates attachment to extracellular
640 matrix proteins collagen type iv and laminin as well as collagen type i.
641 Infection and Immunity 68:5218-5224.

642 27. Singh KV, Nallapareddy SR, Sillanpaa J, Murray BE. 2010. Importance of the
643 collagen adhesin ace in pathogenesis and protection against *Enterococcus*
644 *faecalis* experimental endocarditis. PLoS Pathogens 6:e1000716.

645 28. Allen BL, Katz B, Hook M. 2002. *Streptococcus anginosus* adheres to
646 vascular endothelium basement membrane and purified extracellular matrix
647 proteins. Microbial Pathogenesis 32:191-204.

648 29. Gong Q, He L, Liu Y, Zhong J, Wang S, Xie M, Sun S, Zheng J, Xiang L,
649 Ricupero CL, Nie H, Ling J, Mao JJ. 2017. Biomaterials selection for dental
650 pulp regeneration, p 159-173. *In* Ducheyne P (ed), Comprehensive
651 biomaterials II, 2nd ed. Elsevier, Oxford.

652 30. Guzmàn CA, Pruzzo C, Li Pira G, Calegari L. 1989. Role of adherence in
653 pathogenesis of *Enterococcus faecalis* urinary tract infection and endocarditis.
654 Infection and Immunity 57:1834-1838.

655 31. Park OJ, Han JY, Baik JE, Jeon JH, Kang SS, Yun CH, Oh JW, Seo HS, Han
656 SH. 2013. Lipoteichoic acid of *Enterococcus faecalis* induces the expression
657 of chemokines via tlr2 and pafr signaling pathways. J Leukoc Biol 94:1275-84.

658 32. de Oliveira LA, Barbosa SV. 2003. The reaction of dental pulp to *Escherichia*
659 *coli* lipopolysaccharide and *Enterococcus faecalis* lipoteichoic acid. Brazilian
660 Journal of Microbiology 34:179-181.

661 33. Baik JE, Ryu YH, Han JY, Im J, Kum KY, Yun CH, Lee K, Han SH. 2008.
662 Lipoteichoic acid partially contributes to the inflammatory responses to
663 *Enterococcus faecalis*. J Endod 34:975-82.

664 34. Wang S, Liu KUN, Seneviratne CJ, Li X, Cheung GSP, Jin L, Chu CH, Zhang
665 C. 2015. Lipoteichoic acid from an *Enterococcus faecalis* clinical strain
666 promotes tnf-α expression through the nf-κb and p38 mapk signaling
667 pathways in differentiated thp-1 macrophages. Biomedical Reports 3:697-702.

668 35. Jontell M, Gunraj MN, Bergenholtz G. 1987. Immunocompetent cells in the
669 normal dental pulp. J Dent Res 66:1149-53.

670 36. Okiji T, Jontell M, Belichenko P, Dahlgren U, Bergenholtz G, Dahlstrom A.
671 1997. Structural and functional association between substance p- and
672 calcitonin gene-related peptide-immunoreactive nerves and accessory cells in
673 the rat dental pulp. J Dent Res 76:1818-24.

674 37. Jontell M, Okiji T, Dahlgren U, Bergenholtz G. 1998. Immune defense
675 mechanisms of the dental pulp. Crit Rev Oral Biol Med 9:179-200.

676 38. Chivatxaranukul P, Dashper SG, Messer HH. 2008. Dentinal tubule invasion
677 and adherence by *Enterococcus faecalis*. International Endodontic Journal
678 41:873-882.

679 39. Veerayutthwilai O, Byers MR, Pham TT, Darveau RP, Dale BA. 2007.
680 Differential regulation of immune responses by odontoblasts. Oral Microbiol
681 Immunol 22:5-13.

682 40. Durand SH, Flacher V, Romeas A, Carrouel F, Colomb E, Vincent C, Magloire
683 H, Couble ML, Bleicher F, Staquet MJ, Lebecque S, Farges JC. 2006.
684 Lipoteichoic acid increases tlr and functional chemokine expression while
685 reducing dentin formation in *in vitro* differentiated human odontoblasts. J
686 Immunol 176:2880-7.

687 41. Jiang HW, Zhang W, Ren BP, Zeng JF, Ling JQ. 2006. Expression of toll like
688 receptor 4 in normal human odontoblasts and dental pulp tissue. J Endod
689 32:747-51.

690 42. Paster BJ, Boches SK, Galvin JL, Ericson RE, Lau CN, Levanos VA,
691 Sahasrabudhe A, Dewhirst FE. 2001. Bacterial diversity in human subgingival
692 plaque. J Bacteriol 183:3770-83.

693 43. Kumar S. 2012. Textbook of microbiology, p 251, 1st ed. Jaypee Brothers
694 Medical Publishers, London, UK.

695 44. Bancroft JD, Gamble M. 2008. Microorganisms, p 312, Theory and practice of
696 histological techniques, 8th ed. Churchill Livingstone, London, UK.

45. Bustin SA, Benes V, Garson JA, Hellemans J, Huggett J, Kubista M, Mueller R, Nolan T, Pfaffl MW, Shipley GL, Vandesompele J, Wittwer CT. 2009. The MIQE guidelines: Minimum information for publication of quantitative real-time pcr experiments. Clin Chem 55:611-22.

46. Livak KJ, Schmittgen TD. 2001. Analysis of relative gene expression data using real-time quantitative PCR and the 2(-delta delta c(t)) method. Methods 25:402-8.

47. Andersen CL, Jensen JL, Orntoft TF. 2004. Normalization of real-time quantitative reverse transcription-pcr data: A model-based variance estimation approach to identify genes suited for normalization, applied to bladder and colon cancer data sets. Cancer Res 64:5245-50.

48. Smith EL, Locke M, Waddington RJ, Sloan AJ. 2010. An *ex vivo* rodent mandible culture model for bone repair. Tissue Eng Part C Methods 16:1287-96.

49. Xing W, Deng M, Zhang J, Huang H, Dirsch O, Dahmen U. 2009. Quantitative evaluation and selection of reference genes in a rat model of extended liver resection. J Biomol Tech 20:109-115.

50. Harrington J, Sloan AJ, Waddington RJ. 2014. Quantification of clonal heterogeneity of mesenchymal progenitor cells in dental pulp and bone marrow. Connective Tissue Research 55:62-67.

51. Seol D, Choe H, Zheng H, Jang K, Ramakrishnan PS, Lim T-H, Martin JA. 2011. Selection of reference genes for normalization of quantitative real-time PCR in organ culture of the rat and rabbit intervertebral disc. BMC Research Notes 4:1-8.

721 52. Langnaese K, John R, Schweizer H, Ebmeyer U, Keilhoff G. 2008. Selection
722 of reference genes for quantitative real-time PCR in a rat asphyxial cardiac
723 arrest model. BMC Molecular Biology 9:53-53.
724 53. Lardizábal MN, Nocito AL, Daniele SM, Ornella LA, Palatnik JF, Veggi LM.
725 2012. Reference genes for real-time PCR quantification of microrna and
726 messenger RNAs in rat models of hepatotoxicity. PLoS ONE 7:e36323.
727 54. Qiang L, Lin HV, Kim-Muller JY, Welch CL, Gu W, Accili D. 2011.
728 Proatherogenic abnormalities of lipid metabolism in SirT1 transgenic mice are
729 mediated through creb deacetylation. Cell metabolism 14:758-767.
730

731 **Figure legends**

732 Fig. 1: Growth curves of (A) *E. faecalis*, (B) *S. anginosus*, *E. faecalis* and *S.*
733 *anginosus* combined at a ratio of (C) 50:50 and (D) 90:10 respectively. Mean values
734 of three experimental repeats shown with error bars indicating standard deviation.
735

736 Fig. 2: Gram stain of tooth slices infected with (A) *E. faecalis*, (B) 50:50 *S.*
737 *anginosus : E. faecalis* and (C to E) 90:10 *S. anginosus : E. faecalis*. Arrows
738 highlight areas of bacterial attachment, P represents dental pulp, D represents
739 dentine and S represents soft tissue surrounding the tooth. Representative images
740 of three experimental repeats shown.
741

742 Fig. 3: Localisation of bacterial attachment by fluorescent microscopy for tooth slices
743 infected with: (A) No bacteria control, (B) *E. faecalis,* (C) *S. anginosus,* (D) 50:50 *S.*
744 *anginosus : E. faecalis* and (E) 90:10 *S. anginosus : E. faecalis*. P represents the
745 dental pulp, O the odontoblast region and D the dentine. Representative images of

three experimental repeats shown. (F) Bacterial coverage as quantified by area of fluorescence relative to total pulp area (*p≤0.05, **p≤0.01 and ***p≤0.001). Mean values of three experimental repeats shown with error bars indicating standard error of the mean.

Fig. 4: (A) Viable cells counted per mm^2 of pulp. Tooth slices infected with *E. faecalis* and *S. anginosus*, both alone and in combination after 24 hours all resulted in a significant reduction in viable cell number in the pulp when compared to the non-infected control (*p≤0.05). Mean values of three experimental repeats shown with error bars indicating standard error of the mean. Fold change in (B) TNF-α and (C) IL-1β gene expression as a result of *E. faecalis* and *S. anginosus* infections, alone and in combination (*p≤0.05, **p≤0.01 compared to control samples and $^{+}$p≤0.05 and $^{++}$p≤0.01). Mean values of three experimental repeats shown with error bars indicating standard error of the mean. (D) Immunohistochemistry of TNF-α and IL-1β for control samples and tooth slices infected with *S. anginosus, E. faecalis*, 50:50 *S. anginosus : E. faecalis* and 90:10 *S. anginosus : E. faecalis*, Representative images of three experimental repeats shown.

Fig.5: Fold change in (A) TNF-α and (B) IL-1β gene expression relative to β–actin as a result of treating tooth slices with *E. faecalis* supernatant and heat-killed *E. faecalis* (*p≤0.05 compared to control samples). Mean values of three experimental repeats shown with error bars indicating standard error of the mean. (C) Immunohistochemistry of TNF-α and IL-1β for control samples and tooth slices infected with *E. faecalis* supernatant and heat-killed *E. faecalis.* Representative images of three experimental repeats shown.

Fig. 1

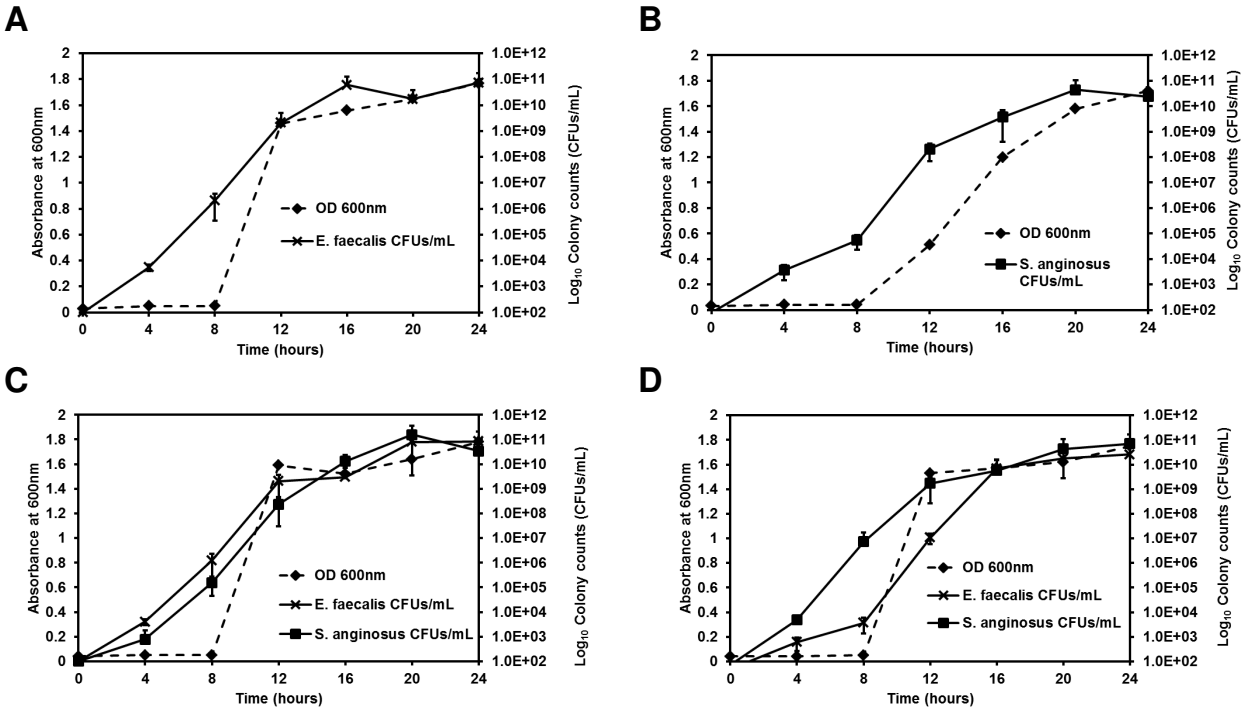

Fig. 2

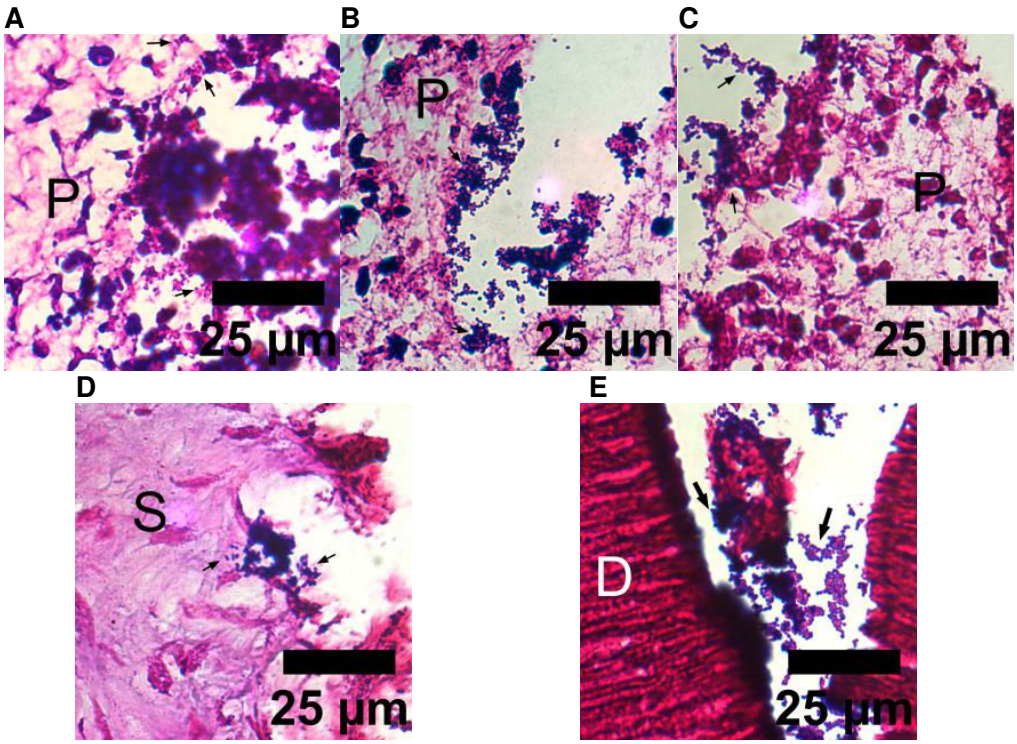

Fig. 3

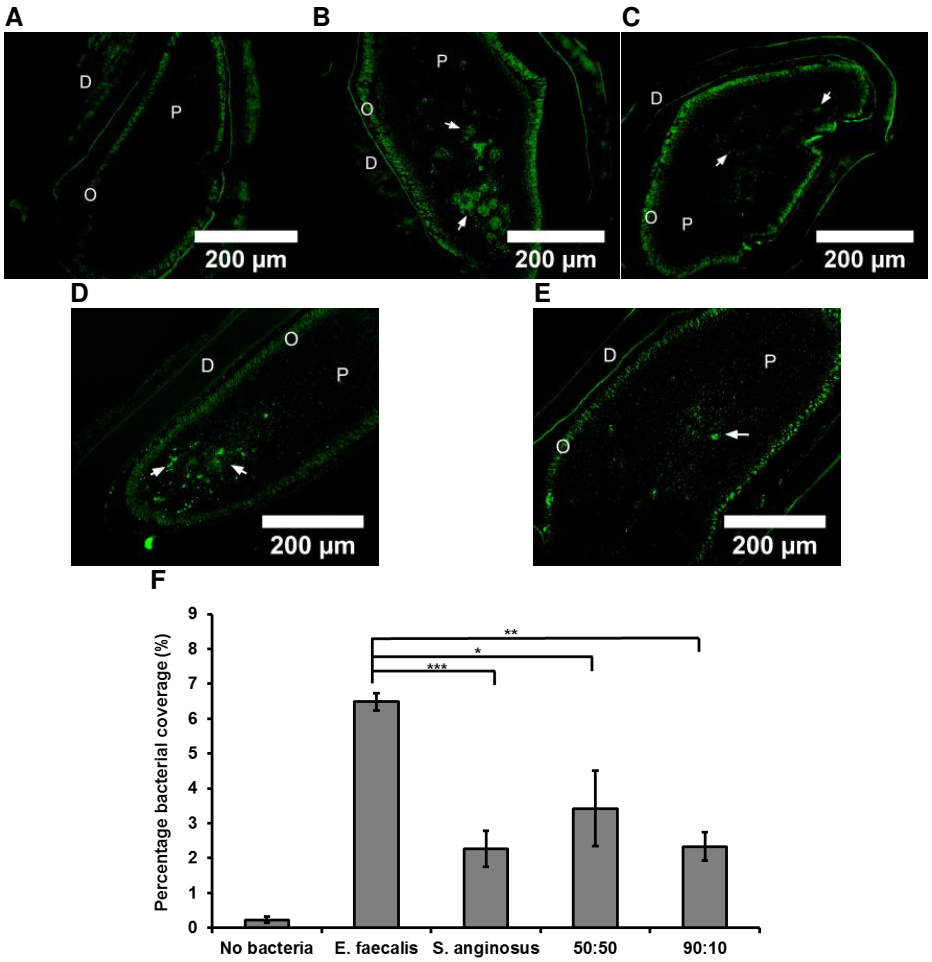

Fig. 4

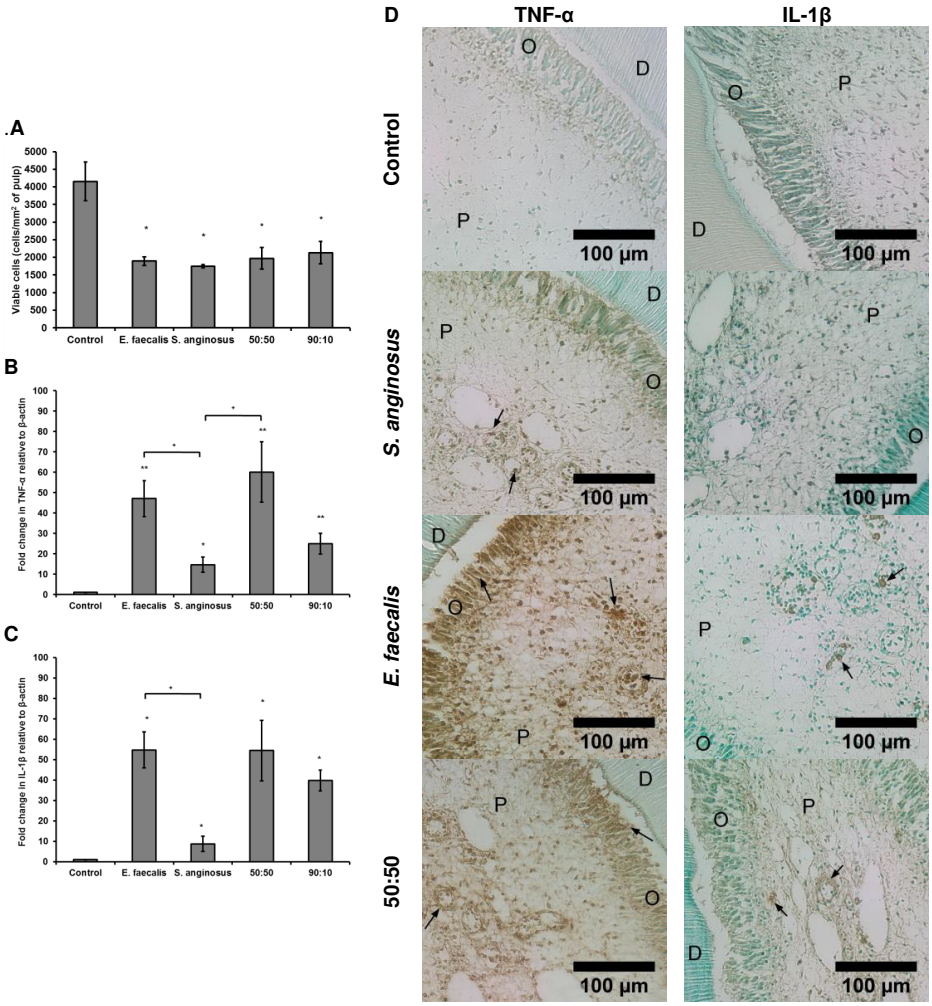

Fig. 5

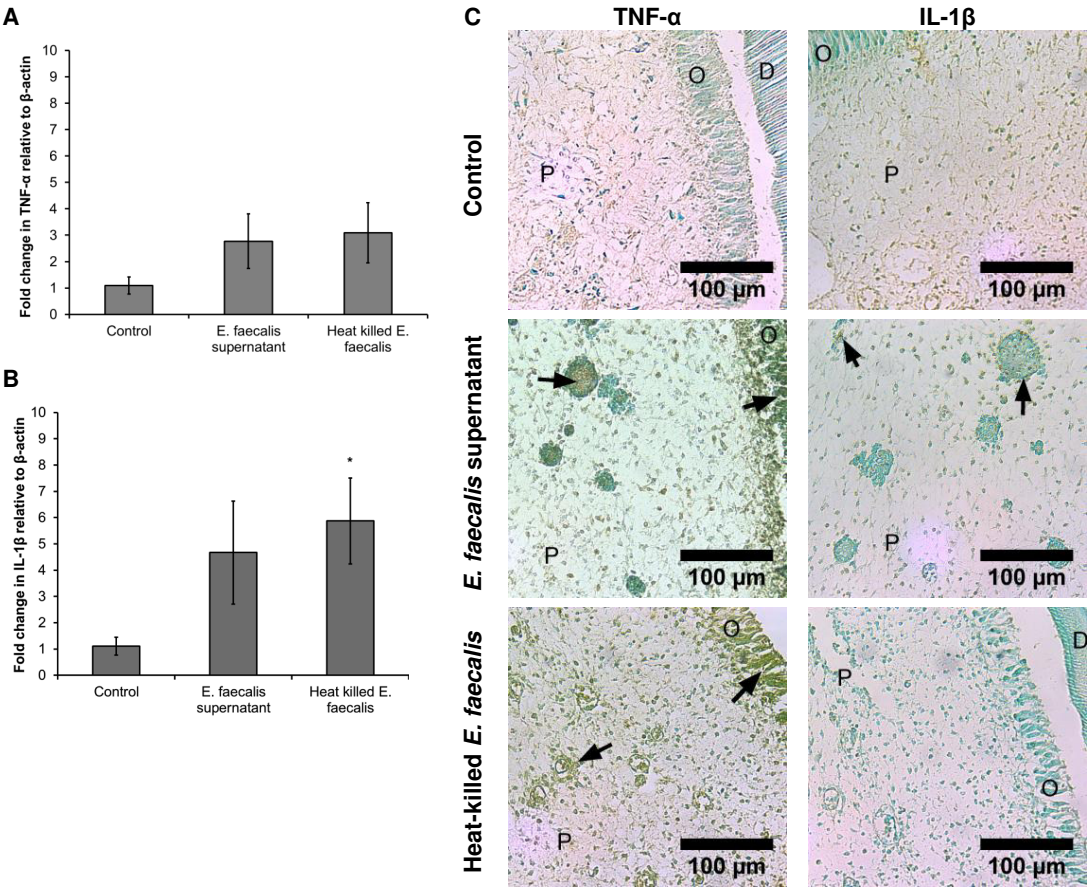

Table 1: Growth rates during the log phase of *S. anginosus* and *E. faecalis* alone and in combination at ratio of 50:50 and 90:10 respectively.

	Average growth rate during log phase (CFUs/mL per hour)	**Standard deviation**
E. faecalis (alone)	1.51	0.20
S. anginosus (alone)	2.00	0.25
E. faecalis (50:50)	1.62	0.10
S. anginosus (50:50)	1.53	0.14
E. faecalis (90:10)	1.98	0.12
S. anginosus (90:10)	1.57	0.12

Table 2: Primer sequences used for qPCR analysis

Gene	Primer sequence (5'-3')	Product length (Bp)	Melting temperature (°C)	Efficiency (%)	Source
Glyceraldehyde 3-phosphate dehydrogenase (GAPDH - NM_017008.4)	Forward – GCA AGA GAG AGG CCC TCA G Reverse – TGT GAG GGA GAT GCT CAG TG	74	61.0 59.4	106.37	(48)
Beta-actin (β-actin - NM_031144.3)	Forward – TGA AGA TCA AGA TCA TTG CTC CTC C Reverse – CTA GAA GCA TTT GCG GTG GAC GAT G	155	60.69 64.37	108.56	(49)
Hypoxanthine Phosphoribosyltransferase 1 (HPRT-1 - NM_012583.2)	Forward – TGT TTG TGT CAT CAG CGA AAG TG Reverse – ATT CAA CTT GCC GCT GTC TTT TA	66	60.24 59.43	91.71	(50)
Ribosomal Protein L13a (RPL13a - NM_173340.2)	Forward – GGA TCC CTC CAC CCT ATG ACA Reverse – CTG GTA CTT CCA CCC GAC CTC	131	61.8 63.7	99.99	(51)
18s ribosomal RNA (18s rRNA – V01270)	Forward – AAA CGG CTA CCA CAT CCA AG Reverse – TTG CCC TCC AAT GGA TCC T	159	57.3 56.7	90.22	(52)
Tumor necrosis factor alpha (TNF-α - NM_012675.3)	Forward – AAA TGG GCT CCC TCT CAT CAG TTC Reverse – TCT GCT TGG TGG TTT GCT ACG AC	111	62.7 62.4	90.28	(53)
Interleukin 1 beta (IL-1β - NM_031512.2)	Forward – ATG CCT CGT GCT GTC TGA CCC ATG TGA G Reverse – CCC AAG GCC ACA GGG ATT TTG TCG TTG C	135	70.06 70.16	94.80	